JOURNAL OF VIROLOGY, June 1975, p. 1487-1497

Vol. 15, No. 6
Printed in U.S.A.

# Anatomy of Herpes Simplex Virus DNA

## II. Size, Composition, and Arrangement of Inverted Terminal Repetitions

SAMUEL WADSWORTH, ROBERT J. JACOB, AND BERNARD ROIZMAN*

*Departments of Microbiology and Biophysics and Theoretical Biology, University of Chicago, Chicago Illinois 60637*

Received for publication 12 February 1975

Electron microscope studies on self-annealed intact single strands and on partially denatured molecules show that herpes simplex virus 1 DNA consists of two unequal regions, each bounded by inverted redundant sequences. Thus the region $L$ (70% of the contour length of the DNA) separates the left terminal region $a_1b$ from its inverted repeat $b'a'_1$, each of which comprises 6% of the DNA. The region $S$ (9.4% of DNA) separates the right terminal region $ca_s$ (4.3% of the DNA) from its inverted repeat $a'_sc'$. The regions of the two termini which are inverted and repeated internally differ in topology. Thus, $ca_s$ is guanine plus cytosine rich, whereas only the terminal 1% of the $a_1b$ region, designated as subregion $a_1$, is guanine plus cytosine rich.

The DNAs of herpes simplex viruses 1 and 2 (human herpesvirus 1 and 2, HSV-1 and HSV-2) are linear duplex molecules approximately $10^8$ in molecular weight (15). Although HSV-1 and HSV-2 DNAs differ only slightly in base composition, (66 and 68 guanine plus cytosine [G+C] mol%, respectively, [8, 15]), they show approximately 50% homology with good (85%) matching of base pairs (16). An unusual feature of the DNAs is that only 10 to 30% of the strands remain intact on denaturation with alkali (6, 15, 19, 24); the rest of the DNA appears to be fragmented. Although the fragmentation of DNA was also observed upon denaturation with formamide (S. Wadsworth and B. Roizman, unpublished data), the presence of ribonucleotides in the DNA might be a contributing factor to the fragmentation of DNA by alkali (11). Current studies show that approximately 40% of HSV-1 DNA is represented in the form of mRNA on polyribosomes during infection (18); concurrently at least 48 viral polypeptides accounting for about 85 to 90% of the DNA sequences represented in polyribosomes have been identified (12).

The objectives of the studies on viral DNA are to map the functions expressed by the virus. Analyses of the products of restriction enzyme cleavage of DNA will be dealt with elsewhere (G. Hayward, N. Frenkel, and B. Roizman, Proc. Natl. Acad. Sci. U.S.A., in press). This paper deals with electron microscope studies on denatured and partially denatured HSV-1 DNA. Pertinent to the data reported in this paper are the observations by P. Sheldrick and N. Berthelot (Cold Spring Harbor Symp. Quant. Biol., in press) that the termini of intact single strands of DNA from several strains of HSV-1 and HSV-2 anneal to internal inverted sequences. Moreover, Sheldrick and Berthelot and R. Grafstrom, J. Alwine, W. Steinhart, and C. Hill (Cold Spring Harbor Symp. Quant. Biol., in press) reported circularization of DNA digested with exonucleases, indicative of terminal redundancy in HSV DNA. These studies led to the conclusion that HSV-1 DNA contains terminal redundant regions which are inverted and repeated internally (Sheldrick and Berthelot, Cold Spring Harbor Symp. Quant. Biol., in press).

## MATERIALS AND METHODS

**Cells and virus.** The procedure for maintenance and infection of HEp-2 cells was described elsewhere (21). The virus strains used in this study were HSV-1 (F1) and HSV-1 (Justin). HSV-1 (F1) was isolated from a facial lesion (5) and passaged a maximum of four times at low multiplicity in HEp-2 cells. The properties of the HSV-1 (F1) virion and of cells infected with this virus were published in detail elsewhere (10). HSV-1 (Justin) was obtained from Albert Sabin. Prior to use, the virus was plaque purified as described elsewhere (N. Frenkel, R. J. Jacob, R. W. Honess, G. Hayward, H. Locker and B. Roizman, J. Virol., in press). The virus contained in a plaque was propagated once at a multiplicity of $10^{-6}$ PFU/cell and subsequently at $10^{-4}$ PFU/cell. The stock of virus obtained at this passage was designated as passage 0 (P0). Both HSV-1 (F1) and HSV-1 (Justin P0) stock were free of defective viral DNA and exhibited none of the biologic properties associated with populations contain-

ing defective virions (Frenkel et al., J. Virol., in press).

**Purification of viral DNA.** HSV-1 (F1) DNA was prepared from cells infected at a multiplicity of 5 PFU/cell. HSV-1 (Justin) DNA was prepared from cells infected at a multiplicity of 0.01 PFU of P0/cell. In both instances the cells were labeled with [methyl-$^3$H]thymidine (1 to 5 μCi/ml of medium, specific activity 40 to 60 Ci/mmol, New England Nuclear, Cambridge, Mass.). DNA was extracted from virions purified from cytoplasmic extracts (23) or from purified nucleocapsids (7). Briefly, virions or nucleocapsids were disrupted with 1% sarkosyl (ICN/K and K Laboratories, Inc., Cleveland, Ohio) and 0.5% sodium dodecyl sulfate. The DNA was then extracted gently with phenol and with chloroform-2% isoamyl alcohol. In some preparations the DNA was then precipitated with alcohol, redissolved in 10mM Tris-hydrochloride (pH 8)-1 mM EDTA (TE buffer), and dialyzed at 4 C against the same buffer. In others, the alcohol precipitation step was omitted, and the DNA was dialyzed directly against TE buffer.

**Isolation of intact strands of HSV-1 DNA.** Viral DNA was denatured with either formamide or alkali. In the first instance, DNA in TE buffer containing 97% (vol/vol) formamide was heated at 60 C for 10 min and then centrifuged in a SW41 rotor at 30,000 rpm and 18 C for 75 to 90 min in a 5 to 20% (wt/wt) sucrose density gradient prepared in neutral DNA buffer (15). Denaturation with alkali was done by one of two techniques.

In some experiments a 5 to 20% (wt/wt) sucrose density gradient prepared in neutral DNA buffer (15) was overlayed with 0.3 ml of 0.3 N NaOH. The DNA was then placed on top of the NaOH layer and centrifuged as described above. In other experiments, the DNA was denatured with 0.1 N NaOH and either neutralized first or directly layered on top of the sucrose density gradient. The fractions of the gradients containing intact strands, determined from cocentrifugation studies with denatured intact $^{14}$C-labeled T4 DNA, were harvested and dialyzed at 4 C against TE buffer. Approximately 10 to 15% of total DNA was recovered as intact strands.

**Digestion of HSV DNA with lambda exonuclease.** The lambda exonuclease, purified from *Escherichia coli* 1100 ($\lambda T_{11}$) (20), was the kind gift of Marc Rhoades, Department of Biology, Johns Hopkins University. Digestion was carried out in 0.067 M glycine-KOH (pH 9.6)-0.003 M $MgCl_2$ at room temperature and was stopped by the addition of 1/10 volume of 20X standard saline citrate.

**Self-annealing of intact strands or of λ exonuclease digests of HSV DNA.** The intact strands or λ exonuclease-digested DNA, at concentrations of 1 μg/ml or less, were annealed in 66% (vol/vol) formamide in TE buffer at 24 C for approximately 3 h. The mixture was then either diluted to 40% formamide for microscopy or dialyzed against TE buffer at 4 C for storage.

**Partial denaturation of DNA by alkaline formaldehyde.** Prior to partial denaturation, portions of the DNA preparations were spread in a protein monolayer (17). The contour length of the DNA was then measured to verify size and configuration. Partial denaturation was done by the method of Inman and Schnös (13). Specifically, a 20 μliter sample of DNA (40 to 60 μg/ml) was mixed with 20 μliters of alkaline formaldehyde (0.12M $Na^+$, 6.4 M formaldehyde) and allowed to react for 2 to 40 min at 25 C. The proportion of NaOH and sodium carbonate in the alkaline formaldehyde stock solution required to yield the desired pH (between 11.20 ± 0.02 and 11.60 ± 0.02) was determined from mixtures of alkaline formaldehyde and the solvent of the DNA solution. The reproducibility of the strand separation patterns and the fact that the extent of separation was related to pH in this and a prior study (14) indicate that no significant change in pH occurred during the reaction of the DNA with alkaline formaldehyde.

**Preparation of DNA-cytochrome c films.** Two preparative procedures were used to prepare DNA-cytochrome *c* film.

(i) The aqueous method of spreading DNA in a cytochrome *c* film (17) was used for partially denatured DNA molecules. The alkaline formaldehyde reaction was stopped at the appropriate time (see below) by transferring 20 μliters of the reaction mixture to 180 μliters of ice-cold spreading solution consisting of 20 μliters of 0.1 M acetic acid, 140 μliters of 1 M ammonium acetate, and 20 μliters of cytochrome *c* (1 mg/ml; Calbiochem, Elk Grove Village, Ill.), pH 5.0 to 5.2 (17). This spreading solution was used for both alkaline formaldehyde-reacted material and for unreacted DNA which served as a control. After 2 min, 0.1 ml was spread over the surface of a 0.3 M ammonium acetate solution adjusted to pH 5.5 with acetic acid. The DNA-cytochrome *c* film was immediately transferred to parlodion-coated copper grids by surface contact and stained with uranyl acetate in acetone (9).

(ii) The formamide method of spreading DNA in a cytochrome *c* film (4) was used for the visualization of the self-annealed intact DNA strands. This method utilizes a spreading solution consisting of 40% (vol/vol) formamide and 0.1 mg of cytochrome *c* per ml in 0.1 M Tris-hydrochloride (pH 8.6)-0.01 M EDTA and a hypophase containing 10% formamide in 0.01 M Tris-hydrochloride (pH 8.6)-0.001 M EDTA. A 50-μliter sample of spreading solution was allowed to run down a glass slide pretreated with ammonium acetate to the surface of the hypophase. The film was allowed to stand for 1 min and then transferred to parlodion-coated copper grids and stained with uranyl acetate in 90% ethanol (4).

**Electron microscopy of DNA.** The grids were shadowed with platinum-paladium and examined in an AEI EM 6B electron microscope at 60 kV. The electron micrographs were taken at magnifications ranging from 5,000 to 20,000×.

**Contour mapping and profile measurements.** The micrographs were rear projected on a screen attached to a Graf Pen (Science Accessories Corp., Southport, Conn.) interfaced to a digital computer (General Automation SP-16/45). Extended molecules were measured and traced; broken and entangled DNAs were neglected. DNA lengths were computed relative to measurements of cross-line grating replicas

(2,160 lines/mm, E. Fullam, Inc. Schnectedy, N.Y.) photographed at the same magnification or to measurements of $\phi$X174 circular DNA (gift of P. Achey) and PM2 form II DNA (gift of J. Lebowitz) admixed with HSV-1 DNA immediately before spreading.

## RESULTS

**Electron microscopy of self-annealed intact strands of HSV-1 DNA.** Electron microscope studies of self-annealed DNA revealed three kinds of molecules of particular interest. These were as follows.

(i) Molecules designated as type A are ones in which one terminus annealed to an internal region to form a structure consisting of a small single-stranded loop, a short double-stranded region, and a long single-stranded tail (Fig. 1). We have designated the terminal region anneal-

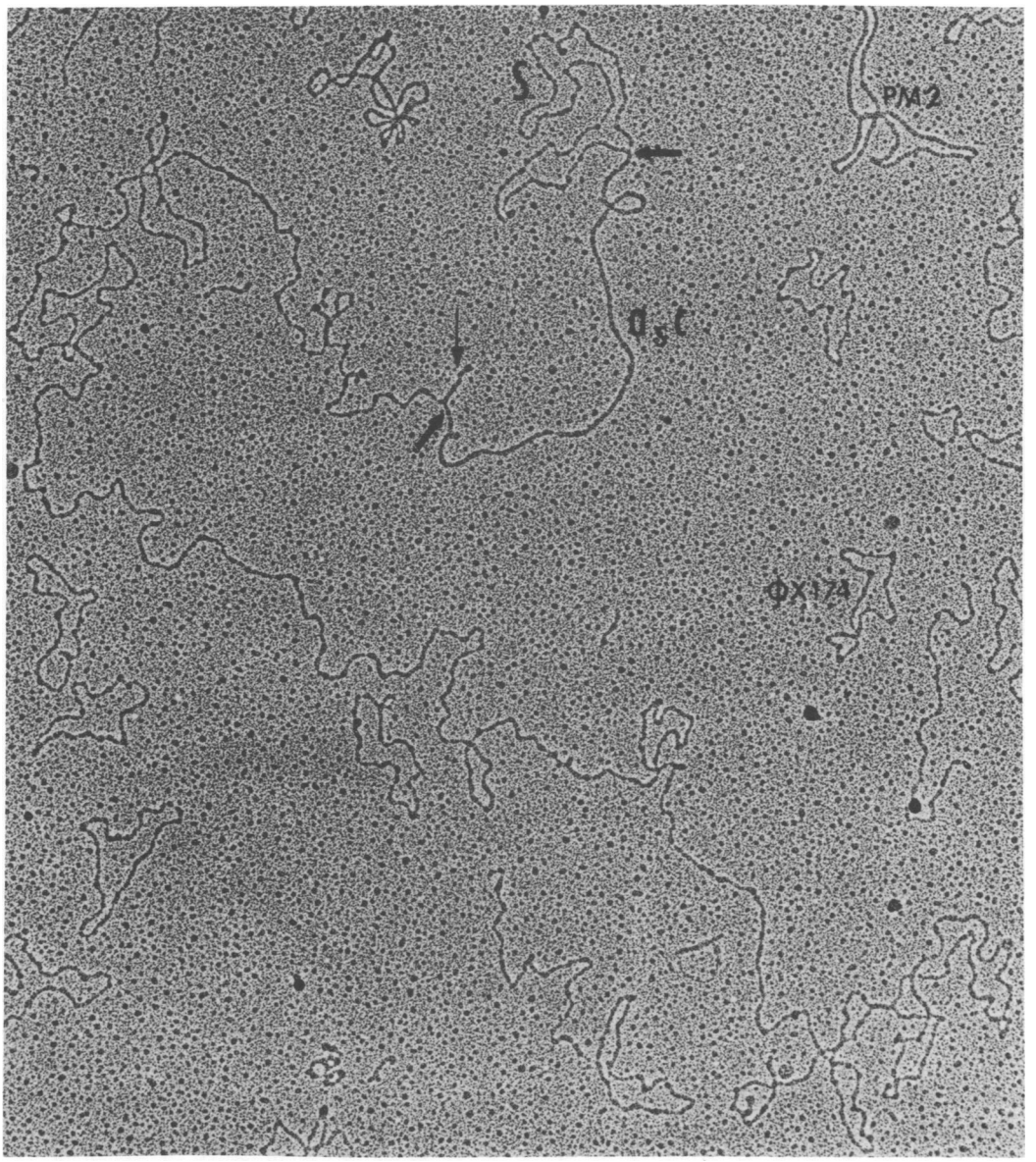


FIG. 1. *Electronmicrograph of self-annealed intact strand of HSV-1 (F1) DNA demonstrating the a,c duplex region and the S loop. Arrows indicate the boundaries of the duplex a,c region. The spur (see text) is indicated by the thin arrow. PM2 and ΦX174 DNA served as magnification standards for double-stranded and single-stranded DNAs, respectively.*

ing to the internal inverted repeat as $ca_s$, and shall refer to it as the right end of the molecule ending in the sequence $a_s$. The internal inverted region complementary to the right terminus shall be designated as $a'_sc'$. The region between $a'_sc'$ and $ca_s$ which is contained in the single-stranded loop was designated as $S$. A characteristic feature of many but not all of these molecules was the presence of a small spur approximately 300 to 500 bases long at the end of the double-stranded region (Fig. 1).

(ii) Molecules designated as type B are ones in which both termini annealed to internal inverted sequences to yield a structure consisting of a large and a small single-stranded loop bridged by a double-stranded region (Fig. 2). Since the small loop could not be differentiated from the loop observed in type A molecule, with respect to size, we shall also refer to it as $S$. The sequences present in the left terminus complementary to the internal inverted repeat shall be designated as $a_1b$, those of the complementary region become $b'a'_1$, and the region bridging the terminal sequences and their inverted repeats as $L$. The internal region containing the inverted, complementary regions becomes, from left to right, $b'a'_1a'_sc'$. It is noteworthy that approximately 30% of the type B molecules also showed a spur. The length of the region from the spur to the small loop corresponded in length to the double-stranded region of type A molecules.

(iii) Molecules designated as type C consist of largely single-stranded structures whose ends seemed entangled in a bush. These were similar to those described by Sheldrik and Berthelot (Cold Spring Harbor Symp. Quant. Biol., in press). Frequently either the $ca_s$ or the $a_1b$ duplex regions with the associated $S$ or $L$ loop could be discerned, but generally the boundaries were too ill defined to be measured.

The type A and B molecules constituted 60% of self-annealed intact strands of HSV-1 (F1). Type C accounted for another 12%. Histograms of the size distributions of the regions $S$, $L$, $ba_1$, $a_sc$, and $ca_s$ in type A and B molecules from several experiments are shown in Fig. 3.

The mean sizes and standard deviations are listed in Table 1. Two points should be made in connection with these measurements. First, the size of the region $a_1b$ was determined by subtracting from measurements of $ba_1$ $a_sc$, the size of the $ca_s$ region.

Second, although the terminal regions $a_1b$ and $ca_s$ are similar in size (6.0 versus 4.3% of the DNA), they are clearly not identical in size. It is noteworthy, moreover, that the terminal regions ($a_1b$, and $ca_s$) and their inverted repeats ($b'a'_1a'_sc'$) constitute more than 20% of the length of the DNA.

**Electron microscopy of self-annealed λ exonuclease-digested HSV-1 DNA.** The purpose of these experiments was to demonstrate by still another technique that the terminal regions were inverted and repeated internally. The rationale of the experiments was that if digestion of native HSV-1 DNA with λ 5′ exonuclease was allowed to proceed beyond the internal inverted region, the terminus near the inverted region ($ca_s$) would then be able to anneal to its complement $a'_sc'$. DNA digests were prepared and annealed as described in Materials and Methods and then spread by the formamide-spreading procedure. Figure 4 shows one of several molecules with a terminal loop observed in these preparations. The loop corresponds in size to the $S$ loop shown in Fig. 1 and 2.

**Partial denaturation mapping of HSV-1 DNA.** The extent of partial denaturation of DNA by the alkaline formaldehyde procedure is determined by the average base composition, the pH of the solvent, and the duration of the treatment (13) assuming ionic strength and temperature are held constant. As far as we know, DNAs with a G+C content as high as 66 mol% have not been mapped by partial denaturation, and therefore we had to determine experimentally the conditions which would yield the most informative map. The condition which gave the most extensive denaturation (pH 11.55, 35 min) yielded less than full size molecules held together by short stretches of G+C rich regions. An undesirable feature was the presence of many single-stranded ends either because of nicks or hydrolysis of alkali labile bonds. The conditions which produce least denaturation (pH 11.27, 7 min) yielded molecules showing very minimal strand separation, and these generally furnished little information on the distribution of G+C rich regions in HSV-DNA. Within this range, treatment of HSV-1 DNA at pH 11.48 for 7 min gave the most advanced denaturation profiles without causing fragmentation of the DNA. Figure 5a shows a tracing of a typical denaturation profile of an HSV-1 (F1) DNA molecule under these conditions. Results of analyses of molecules partially denatured in this fashion may be summarized as follows.

(i) The extent of denaturation ranged from 40 to 60% and was accompanied by a shrinkage of up to 30% of the DNA contour lengths.

(ii) All of the partially denatured DNA molecules had several distinct features which per-


FIG. 2. *Electronmicrograph of self-annealed intact strand of HSV-1 (F1) DNA demonstrating the $ba_1a_sc$ duplex region, the S and L loops. Arrows indicate the boundaries of the duplex $ba_1a_sc$ region. The spur is indicated by the thin arrow.*

mitted the construction of an oriented linear array. Specifically, both ends of the molecule terminated in G+C rich sequences. However, the G+C rich stretch at one end (designated as the right end) was longer (1.73 ± 0.12 μm) than that at the left end (0.38 ± 0.07 μm). In addition, all molecules had a long internal G+C rich region (2.39 ± 0.44 μm) close to the right

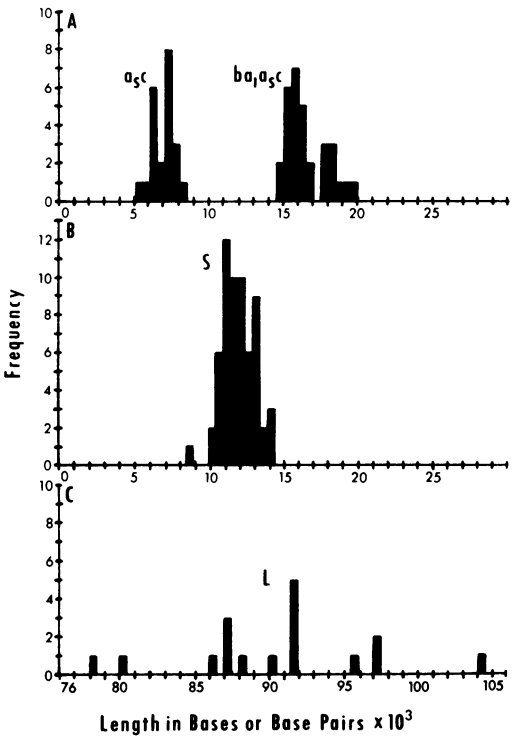


FIG. 3. *Histogram of lengths of the $a_sc$, $ba_1a_sc$, S, and L regions of self-annealed intact strands. Molecules were measured relative to either ΦX174 DNA for single-stranded regions or relative to PM2 DNA for double-stranded regions. The lengths are plotted as bases or base pairs taking a value of 5.8 × $10^3$ bases for single-stranded ΦX174 DNA and 10.8 × $10^3$ base pairs for PM2 DNA. We have no explanation for the apparent bimodality of the lengths of the $ba_1a_sc$ region, but it is interesting to note that the spur, when present (see text), was always observed at the same relative location in $ba_1a_sc$ regardless of the length of this duplex region.*

end. A double loop at the end of the left terminal G+C rich region was present in 80% of the molecules. In the remainder of the molecules a single loop was present. Moreover, a double loop of the same dimensions was usually present to the left of the long internal G+C rich region.

(iii) The regular appearance of several of these features clearly emerges from the linear array of partially denatured HSV-1 (Justin P0) DNA molecules (Fig. 5b). For the construction of the linear array, we corrected for the shrinkage of the denatured sequences by multiplying the contour length of one side of a denatured loop (i.e., one half of the total contour length of the loop) by the ratio of linear densities of double-stranded to single-stranded DNA. The linear density values for double-stranded and single-stranded DNA given by Bujard (3) were 2.15 × $10^6$ and 1.65 × $10^6$ daltons/μm, respectively. The profiles in the array were aligned for maximum overlap of the adenine plus thymine (A+T) rich sequences immediately to the left side of the most regular large internal G+C rich region.

The profiles of the partially denatured DNA

TABLE 1. *Contour lengths and molecular weights of HSV-1 DNA and its subregions*[a]

| Portion of DNA measured | No. of molecules measured | Length relative to PM2 | Length relative to φX174 | Length (μm) | % length of native DNA | Mol wt (× $10^{-6}$) | Length in bases or base pairs (× $10^{-3}$) |
|---|---|---|---|---|---|---|---|
| $ca_s$ | 22 | 0.64 ± 0.06 | | 1.9 ± 0.2[b] | 4.31 ± 0.42 | 4.13 ± 0.4[c] | 6.89 ± 0.67[c] |
| $ba_1a_sc$ | 31 | 1.52 ± 0.12 | | 4.6 ± 0.4[b] | 10.31 ± 0.84 | 9.89 ± 0.81[c] | 16.5 ± 1.4[c] |
| $a_1b$ ($ba_1a_sc$-$ca_s$) | | 0.88 | | 2.7[b] | 6.0 | 5.8[c] | 9.6[c] |
| *S* | 61 | | 2.09 ± 0.19 | 4.2 ± 0.4[b] | 9.41 ± 0.85 | 8.99 ± 0.81[d] | 12.1 ± 1.1[d] |
| *L* | 17 | | 15.6 ± 1.1 | 31.2 ± 0.2[b] | 70.1 ± 4.7 | 67.2 ± 4.5[d] | 90.5 ± 6[e] |
| Intact | 6 | 14.8 ± 0.6 | | 44.7 ± 1.9[b] | 100 ± 4 | 96 ± 4[c] | 160 ± 6[c] |
| Native | 10 | | | 44.5 ± 2.8[f] | | [95.7 ± 6][b] | |

[a] Measurements given as mean ± standard deviation.
[b] Calculated from linear density value of 2.15 × $10^6$ mol wt/μm (3).
[c] Calculated from the mol wt value for PM2 of 6.5 × $10^6$ (10.8 × $10^3$ base pairs).
[d] Due to shrinkage the combined length of the single-stranded region *S* and *L* was less than that predicted from the length of the native molecule less the duplex $ba_1a_sc$. We therefore calculated the lengths of the *S* and *L* regions by subtracting from the length of the native molecule the lengths of the termini and their inverted repeats and distributed the remainder between the *S* and *L* regions in proportion to their respective lengths relative to φX174.
[e] Calculated from the mol wt value of φX174 of 1.7 × $10^6$ (22) (5.8 × $10^3$ bases).
[f] Measured relative to cross-line grating replicas, 2,160 lines/mm.

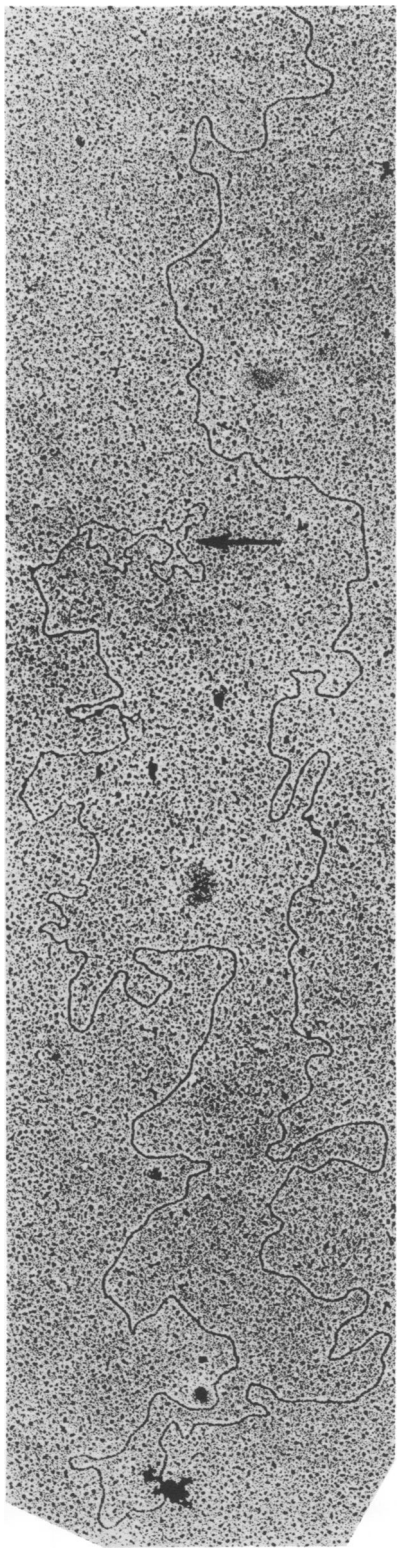

molecules (Fig. 5a and b) show several striking features. First, the internal G+C rich region is approximately the sum of the terminal left and right G+C regions. Second, the A+T rich sequences demarcated by arrows immediately to the left of the internal G+C rich region bear a striking similarity in size and topology to the inverted image of the A+T rich sequences immediately next to the G+C rich stretch at the left terminus (Fig. 6). Third, the overall sizes of the left and right terminal regions whose inverted images appear to be duplicated internally, as well as the size of the region containing the inverted images, correspond respectively to those of the $a_1b$, $ca_s$ and $b'a'_1a'_sc'$ regions obtained from measurements of self-annealed molecules. Lastly, the regions between the left and right termini and their inverted images correspond in size to the $L$ and $S$ regions described earlier in the text. Thus, the ratio of the contour lengths of these regions is 8.5, i.e., in good agreement with the ratio of measurements of the $L$ and $S$ regions shown in Table 1.

(iv) The dimensions of the $a_1b$ and $ca_s$ regions we have accepted are those based on measurements of self-annealed DNA molecules. In the partial denaturation profiles, the boundaries of the $a_1b$ region are easily deduced by comparing the topology of the left terminus with the topology of the DNA sequences immediately to the left of the large internal G+C region. The topology of the right terminus is devoid of distinguishing features. We do not know whether the boundaries of $ca_s$ region are beyond (as shown in Fig. 5a) or just before the first A+T rich loop (as shown in Fig. 5b).

(v) On the basis of the partial denaturation profiles we have designated the terminal G+C rich sequences within the $a_1b$ region as the $a_1$ subregion. Its dimensions ($0.38 \pm 0.07$) correspond to approximately 1% of the total DNA length. A G+C rich stretch of similar length from the right end was arbitrarily designated as the $a_s$ subregion.

## DISCUSSION

The main features of the data presented in this paper may be summarized as follows.

FIG. 4. *Electronmicrograph of λ exonuclease-digested self-annealed DNA. Native DNA was digested with the λ exonuclease to expose the $a_sc$ and $a'_sc'$ regions. The DNA was then annealed in 66% formamide under the same conditions as intact strand annealing and spread for electron microscopy using the formamide spreading technique (4). The S loop is indicated by the arrow. The other end of this molecule, in part single stranded, extends under a grid bar.*

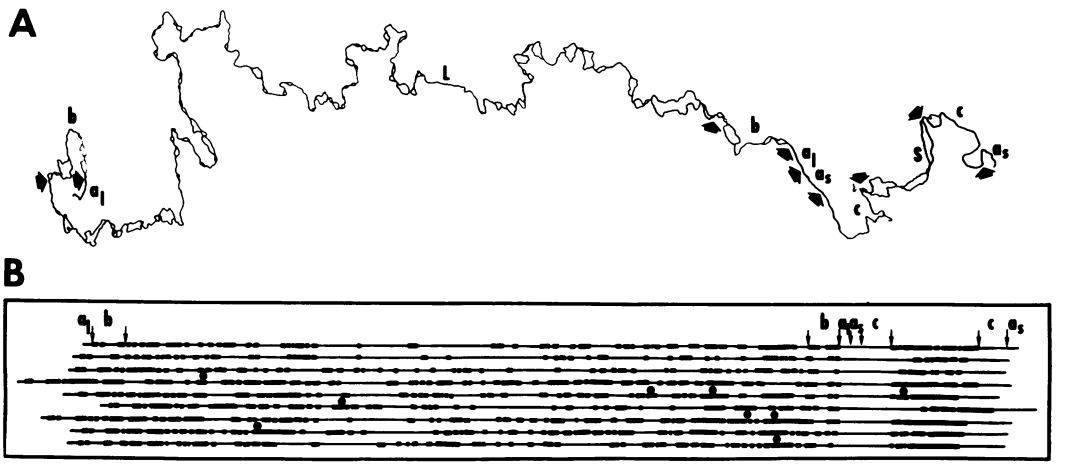


FIG. 5. *(A) Tracing of a partially denatured HSV-1 (F1) DNA molecule. (B) Linear array of partially denatured HSV-1 (P0 Justin) DNA molecules. The dots indicate the positions of broken strands. The denaturation conditions were pH 11.48 for 7 min at 25 C.*

(i) Based on the self annealing of intact strands, we corroborate the findings of Sheldrick and Berthelot (Cold Spring Harbor Symp. Quant. Biol., in press) that inversions of the terminal sequences of HSV-1 DNA are repeated and occupy adjacent positions in the DNA molecule. It should be reiterated that inverted repeats could be demonstrated in at least 60% of intact strands, and that they are not due to the high-buoyant-density species characteristic of HSV-1 defective DNA ($\rho$ = 1.732 g/cm$^3$) (2).

(ii) Our measurements, in contrast to those of Sheldrick and Berthelot (Cold Spring Harbor Symp. Quant. Biol., in press), show that the terminal regions which are inverted are not identical in size: Thus, the inverted region of the right terminus, designated $ca_s$, comprises 4.3% of the DNA, whereas the inverted region of the left terminus, designated $a_1b$, comprises 6.0% of the DNA. Parenthetically, the measurements of the contour lengths of native DNA relative to either PM2 or cross-lined replica gratings yield a molecular weight for native HSV-1 DNA of 96 million, i.e., in good agreement with that obtained by Becker et al. (1) and by our laboratory from velocity sedimentation studies (15).

(iii) The partial denaturation profiles of HSV-1 (F1) and of HSV-1 (Justin P0) DNAs are consistent with the data obtained from the observations and measurements made on self-annealed DNA molecules. Specifically, partial denaturation profiles show that inverted images of both termini were contiguous and located at positions predicted from measurements of self-annealed intact strands. A point of interest to be noted is that whereas the denaturation profiles of the regions $a_1b$, $ca_s$ and of their inverted repeats were consistent and reproducible, this was not the case for the *L* and *S* regions. In part, this might be due to incomplete denaturation of regions with intermediate to low A+T content under the partial denaturation conditions to which these molecules were subjected. In part, however, this might be due to inversions in the *L* and in the *S* regions predicted by restriction endonuclease analyses (B. Roizman, G. Hayward, R. J. Jacob, S. Wadsworth, R. W. Honess, N. Frenkel, and M. Kozak, Proc. Symp. Herpesviruses Oncogenesis IARC, in press) and (G. Hayward, R. J. Jacob, S. Wadsworth, and B. Roizman, manuscript in preparation).

(iv) The partial denaturation profiles set constraints on the extent of possible homology predicted by the studies on terminal redundancy (Grafstrom et al., and Sheldrick and Berthelot) and indicate that the terminal regions $a_1b$ and $ca_s$ are for the most part different. Specifically, the profiles predict that the sequences which could be terminally redundant cannot exceed the size of the terminal G+C rich sequences in the $a_1b$ region of the left terminus. Although the subregion of $a_1b$ designated as $a_1$ comprises approximately 1% of the DNA, and thus is in good agreement with the extent of terminal redundancy reported by Grafstrom et al., the experiments do not allow us to conclude that it is homologous to the corresponding $a_s$

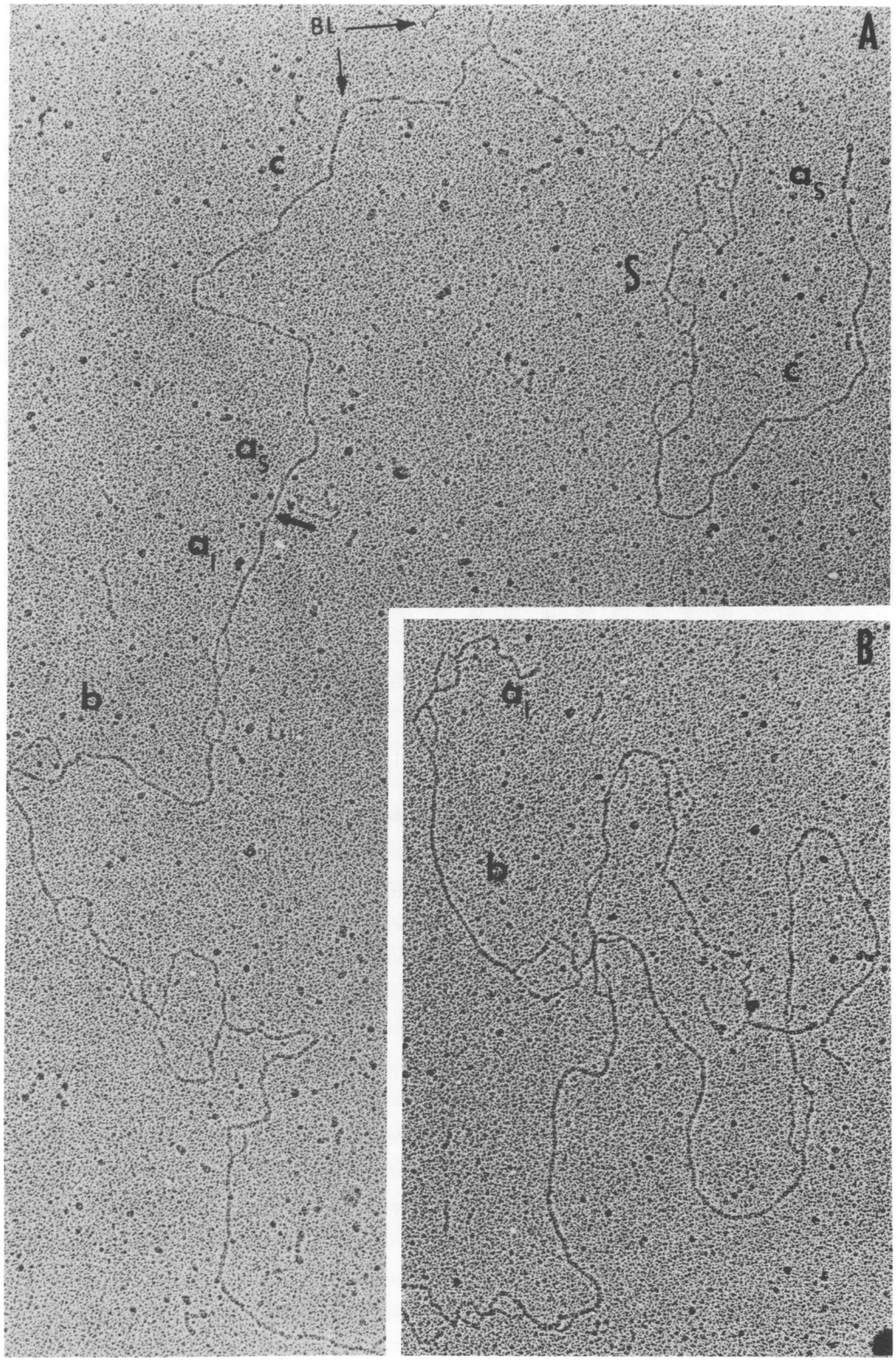


FIG. 6. *Electron micrographs of plaque purified HSV-1 (Justin) DNA partially denatured at pH 11.48 for 7 min at 25 C. (A) Right terminus showing regions $a_sc$, S, and the region $ba_1a_sc$ containing the inverted terminal repetitions. (B) Left terminus of the same molecule. Note correspondence of the region $a_1b$ in (B) with the internally inverted region designated by the same letters and shown in (A).*

sequences of the $ca_s$ region. Our data do indicate, however, that the remainder of the terminal sequences inverted and repeated internally, i.e., subregions *b* and *c*, have different partial denaturation profiles and thus would be predicted to have little homology.

(v) Of special interest bearing on the identity of the terminal $a_1$ and $a_s$ regions and their inverted repeats is the observation of spurs at the $a_1$-$a_s$ joint in self-annealed intact strands. The spur seems to be a small folded structure since it appears more similar to duplex DNA rather than single-stranded DNA. Among the many possible explanations for the spur are the following. First, the terminal $a_s$ may sometimes contain a small set of sequences not present in the internal inverted repeat of this region. Second, the sequences in the region $a_s$ and its internal inverted repeat $a'_s$ may be mismatched, and therefore minor fluctuations in spreading conditions could affect the base pairing of these sequences. Lastly, sequences might be inserted into or deleted from the juncture of the internal inverted subregions $a'_1$ and $a'_s$. Although we cannot differentiate between these and other explanations, cognizance must be taken of the possibility that the homology between terminal *a* regions and their inverted repeats may be discontinuous.

(vi) On the basis of the data presented in this paper, we identified and designated specific regions of HSV-1 DNA. From left to right, the arrangement of the sequences along a single strand are $a_1 b\ L\ b' a'_1\ a'_s c' S\ ca_s$. An examination of this sequence shows that DNA consists of two regions of which the left is comprised of sequences $a_1 b\ L\ b' a'_1$ and the right $a_s' c' S c a_s$. It is also noteworthy that the distribution of G+C rich sequences in the two regions is not the same; thus the G+C rich sequences are more uniformly distributed in the left as compared with the right region. The anatomy of HSV DNA appears to be different from that of any DNA virus of eukaryotic cells reported to date.

## ACKNOWLEDGMENTS

We wish to thank Marc Rhoades for the gift of λ exonuclease, P. Achey for the ΦX174 DNA, and J. Lebowitz for the PM2 DNA. We acknowledge B. Cox and C. S. Chen for the computer programs used in measurements of DNA molecules.

These studies were done under the auspices of the Chicago Cancer Research Center Project (CA-14599), and were aided by grants from the American Cancer Society (VC 10J) and the National Science Foundation (GB 38270) and Public Health Service grant no. CA 08494 from the National Cancer Institute. S. W. is a predoctoral trainee (Public Health Service training grant AI 00238 from the National Institute of Allergy and Infectious Diseases) and R. J. J. is a postdoctoral fellow of the American Cancer Society (PF 972).

## LITERATURE CITED

1. Becker, Y., H. Dym, and I. Sarov. 1968. Herpes simplex virus DNA. Virology **36**:184-192.
2. Bronson, D. L., G. R. Dreesman, N. Biswal, and M. Benyesh-Melnick. 1973. Defective virions of herpes simplex viruses. Intervirology **1**:141-153.
3. Bujard, H. 1970. Electron microscopy of single-stranded DNA. J. Mol. Biol. **49**:125-137.
4. Davis, R. W., M. Simon, and N. Davidson. 1971. Electron microscope heteroduplex methods for mapping regions of base sequence homology in nucleic acids, p. 413-428. *In* L. Grossman and K. Moldave (ed.), Methods in enzymology, vol. XXI. Academic Press Inc., New York.
5. Ejercito, P. M., E. D. Kieff, and B. Roizman. 1968. Characterization of herpes simplex virus strains differing in their effect on social behavior of infected cells. J. Gen. Virol. **3**:357-364.
6. Frenkel, N., and B. Roizman. 1972. Separation of the herpes virus deoxyribonucleic acid duplex into unique fragments and intact strand on sedimentation in alkaline gradients. J. Virol. **10**:565-572.
7. Gibson, W., and B. Roizman. 1972. Proteins specified by herpes simplex virus. VIII. Characterization and composition of multiple capsid forms of subtypes 1 and 2. J. Virol. **10**:1044-1052.
8. Goodheart, C. R., G. Plummer, and J. L. Waner. 1968. Density differences of DNA of herpes simplex virus subtypes 1 and 2. Virology **35**:473-475.
9. Gordon, C. M., and A. K. Kleinschmidt. 1968. High contrast staining of individual nucleic acid molecules. Biochim. Biophys. Acta **155**:305-307.
10. Heine, J. W., R. W. Honess, E. Cassai, and B. Roizman. 1974. Proteins specified by herpes simplex virus. XII. The virion polypeptides of type I strains. J. Virol. **14**:640-651.
11. Hirsch, I., and V. Vonka. 1974. Ribonucleotides linked to DNA of herpes simplex virus type I. J. Virol. **13**:1162-1168.
12. Honess, R. W., and B. Roizman. 1974. Regulation of herpes virus macromolecular synthesis. I. Cascade regulation of the synthesis of three groups of viral proteins. J. Virol. **14**:8-19.
13. Inman, R. B., and M. Schnös. 1970. Partial denaturation of thymine and 5-bromouracil-containing λDNA in alkali. J. Mol. Biol. **49**:93-98.
14. Jacob, R. J., J. Lebowitz, and A. K. Kleinschmidt. 1974. Locating interrupted hydrogen bonding in the secondary structure of PM2 circular DNA by comparative denaturation mapping. J. Virol. **13**:1176-1188.
15. Kieff, E. D., S. L. Bachenheimer, and B. Roizman. 1971. Size, composition, and structure of the DNA of subtypes 1 and 2 herpes simplex virus. J. Virol. **8**:125-132.
16. Kieff, E., B. Hoyer, S. L. Bachenheimer, and B. Roizman. 1972. Genetic relatedness of type 1 and type 2 herpes simplex viruses. J. Virol **9**:738-745.
17. Kleinschmidt, A. K. 1968. Monolayer techniques in electron microscopy of nucleic acid molecules, p. 361. *In* L. Grossman and K. Moldave (ed.), Methods in enzymology, vol. 12B. Academic Press Inc., New York.
18. Kozak, M., and B. Roizman. 1974. Regulation of herpesvirus macromolecular synthesis: nuclear retention of non-translated viral RNA sequences. Proc. Natl. Acad. Sci. U.S.A. **71**:4322-4326.
19. Mossmann, T. R., and J. B. Hudson. 1973. Some properties of the genome of murine cytomegalovirus (MCV). Virology **54**:135-149.
20. Radding, C. M. 1966. Regulation of λ exonuclease. I. Properties of λ exonuclease purified from lysogens of $T_{11}$ and wild type. J. Mol. Biol. **18**:235-250.
21. Roizman, B., and P. G. Spear. 1968. Preparation of

herpes simplex virus of high titer. J. Virol. 2:83-84.
22. Sinsheimer, R. L. 1959. A single stranded deoxyribonucleic acid from bacteriophage ΦX174. J. Mol. Biol. 1:43.
23. Spear, P. G., and B. Roizman. 1972. Proteins specified by herpes simplex virus. V. Purification and structural proteins of the herpes virion. J. Virol. 9:143-159.
24. Wilkie, N. M. 1973. The synthesis and substructure of herpesvirus DNA: the distribution of alkali labile single strand interruptions in HSV-1 DNA. J. Gen. Virol. 21:453-467.